

# Dielectric spectroscopy of plant protoplasts

Koji Asami and Tohru Yamaguchi

Institute for Chemical Research, Kyoto University, Uji, Kyoto 611, Japan

**ABSTRACT** The relative permittivity and conductivity of the mesophyll protoplasts isolated from *Brassica campestris* leaves and *Tulipa gesneriana* petals were measured over a frequency range from 1 kHz to 500 MHz. These protoplasts showed a broad dielectric dispersion, which was composed of three subdispersions, termed  $\beta_1$ -,  $\beta_2$ -, and  $\beta_3$ -dispersion in increasing order of frequency. The three subdispersions were assigned to the Maxwell–Wagner dispersion caused by charging processes at the interfaces of the surface and internal membranes; the plasma membrane, the tonoplast, and the membranes of cytoplasmic organelles (e.g., chloroplasts, granules, etc) primarily contribute to the  $\beta_1$ -,  $\beta_2$ -, and  $\beta_3$ -dispersion, respectively. The whole dielectric dispersion curve was satisfactorily interpreted in terms of a spherical cell model taking a large vacuole and cytoplasmic organelles into account. Using this model the capacitances of the plasma membranes and the tonoplasts were estimated to be 0.6–0.7  $\mu\text{F}/\text{cm}^2$  and 0.9–1.0  $\mu\text{F}/\text{cm}^2$ , respectively.

## INTRODUCTION

When a biological cell is placed in a dc field, opposite electric charges (or ions) are accumulated at the opposing interfaces of the plasma membrane, which separates the cytoplasm from the external medium. The cell thus polarized has apparently large static relative permittivity, ranging from  $10^3$  to  $10^4$ , a phenomenon which is called interfacial polarization. When an ac field instead of a dc field is applied, the permittivity changes as a function of frequency. Such frequency dependence is called the Maxwell–Wagner dispersion and has been extensively studied (see reviews by Schwan, 1957; Cole, 1968; Pethig, 1979; Foster and Schwan, 1986; Takashima, 1989). This type of dielectric dispersion is essentially interpreted in terms of a simple spherical cell model, namely, the single-shell model (Pauly and Schwan, 1959; Hanai et al., 1979).

When measuring a cell that has membrane-bounded cytoplasmic organelles, as is usually the case, we might observe additional dielectric dispersions as predicted from electrical cell models, including intracellular organelles, which are termed the double-shell model (Irimajiri et al., 1978; 1979), and the vesicle inclusion model (Irimajiri et al., 1991). In our previous paper (Asami et al., 1989), this prediction was confirmed with mouse lymphocytes (which have a sizeable nucleus) by means of the “suspension” method in which the dielectric properties of the cells are extracted from their suspension using the appropriate mixture equation. The lymphocytes showed one more dielectric dispersion due to the existence of nucleus in addition to the main one caused at the plasma membrane as was predicted theoretically.

In this paper, we report on the dielectric properties of plant protoplasts with a very large vacuole and a thin cytoplasmic layer, including membrane-bounded organelles, such as chloroplasts and mitochondria, at a high concentration. The plant protoplasts, therefore, are ex-

pected to show the Maxwell–Wagner dispersions caused at the internal membranes. The dielectric properties of plant protoplasts have been studied by the electrorotation method (Arnold and Zimmermann, 1982; Glaser et al., 1983; Gimsa et al., 1985) and by the dielectrophoresis method (Lovelace et al., 1984; Kaler and Jones, 1990). Fuhr et al. (1985) discussed the theoretical effect of the presence of a vacuole on the electrorotation spectra of plant protoplasts. To our knowledge, however, these methods have not succeeded in elucidating the dielectric properties of the intracellular structure in situ. Our purpose is, therefore, to apply the suspension method to this problem.

## MATERIALS AND METHODS

### Preparation of protoplasts

Protoplasts were isolated from *Brassica campestris* leaves and *Tulipa gesneriana* petals by the two-step digestion method of Takebe et al. (1968). The leaves or petals, whose lower or abaxial epidermis was peeled off, were cut into small pieces and were immersed in a digestion mixture containing 0.5% Macerozyme R-10 (Yakult Honsha Co., Ltd., Tokyo) and 0.7 M mannitol. The mixture of the leaves or the petals and the enzyme solution was placed under reduced pressure for a few minutes in order to facilitate penetration of the enzyme solution into the tissues. After digestion for 30 min at 25°C, most of the mesophyll cells were dispersed to the enzyme solution. The cell suspension was filtered through two-layers of cheesecloth to remove the debris and the cells were collected by centrifugation at 100 g for 5 min. Then, the cells were resuspended in another digestion mixture containing 2% Cellulase Onozuka R-10 (Yakult Honsha Co., Ltd.) and 0.7 M mannitol to digest the cell walls. After 1–2 h digestion at 37°C the spherical protoplasts were obtained, and were washed twice with 0.7 M mannitol. The protoplasts were purified by centrifugation (10 min at 120 g) through a two-step density gradient consisting of one solution containing 0.35 M mannitol and 0.35 M sucrose, and the second solution 0.7 M sucrose. Protoplasts collected from the interface between the two steps were washed with 0.7 M mannitol, suspended in a solution containing 20 mM KCl, 10 mM  $\text{CaCl}_2$ , 1 mM  $\text{MgSO}_4$ , 1 mM  $\text{KH}_2\text{PO}_4$ , 10  $\mu\text{M}$  KI, 0.1  $\mu\text{M}$   $\text{CuSO}_4$ , and 635 mM mannitol (pH 5.8), and subjected to dielectric measurements.

### Dielectric measurements

Dielectric measurements are usually carried out with a concentrated cell suspension to ensure accuracy and to eliminate the influence of cell

Address correspondence to Dr. Koji Asami, Institute for Chemical Research, Kyoto University, Gokasho, Uji, Kyoto 611, Japan.

sedimentation (Asami and Hanai, 1992). However, when a concentrated protoplast suspension is transferred into a dielectric chamber with a glass pipette or syringe, the protoplasts are damaged by shearing forces resulting from passage through a glass capillary or needle. To avoid this damage, we used a special dielectric chamber in which protoplasts can be safely concentrated by centrifugation. The chamber was filled with 1 ml of a suspension containing about  $10^6$  protoplasts and was centrifuged at 100 g for 5 min. The protoplasts were accumulated in a small cavity (of about 20  $\mu$ l) between a pair of electrodes at the bottom of the chamber. The chamber with a water jacket was connected to Impedance Analyzers (models 4191A and 4192A; Hewlett-Packard Co., Palo Alto, CA) via a spring clip fixture (model 16092A; Hewlett-Packard Co.); Equivalent capacitance and conductance were measured between 1 kHz and 500 MHz, and were corrected for residual inductance and stray capacitance arising from the chamber and the fixture according to the method of Asami et al. (1984). Judging from the results with salt solutions, the correction was reasonable, except for a continual increase in conductivity above 200 MHz. Even after subtracting the conductivity increment due to the dielectric dispersion of water, a systematic increase in conductivity still remained, which might be due to some instrumental errors. All measurements were carried out at 25°C.

### Calculation of equivalent, homogeneous relative permittivity and conductivity of protoplast

The complex relative permittivity of the protoplast  $\epsilon_c^*$  was calculated from that of the protoplast suspension  $\epsilon_s^*$  according to Hanai's mixture equation (Hanai, 1960).

$$\frac{\epsilon_s^* - \epsilon_c^*}{\epsilon_a^* - \epsilon_c^*} \left( \frac{\epsilon_a^*}{\epsilon_s^*} \right)^{1/3} = 1 - P, \quad (1)$$

where  $P$  is the volume fraction of the protoplasts in the suspension and  $\epsilon_a^*$  is the complex relative permittivity of the external medium. Complex relative permittivity is defined as  $\epsilon^* = \epsilon - j\kappa/\omega\epsilon_0$ , in which  $\epsilon$  is relative permittivity,  $\kappa$  conductivity,  $\epsilon_0$  permittivity of vacuum,  $\omega = 2\pi f$ ,  $f$  frequency and  $j = (-1)^{1/2}$ . The value of  $\epsilon_a^*$  is known from the measurements of the supernatant separated from the protoplast suspension by centrifugation. Since the conductivity of the plasma membranes is assumed to be negligibly small compared with that of the external medium, the value of  $P$  is calculated from the following equation (Irimajiri et al., 1975; Asami et al., 1989).

$$P = 1 - (\kappa_1/\kappa_a)^{2/3}, \quad (2)$$

where  $\kappa_1$  is the limiting conductivity of the suspension at low frequencies and  $\kappa_a$  is the conductivity of the external medium.

## RESULTS

### Morphology of protoplasts

Fig. 1 shows the optical micrographs of the mesophyll protoplasts isolated from *Brassica campestris* leaves and *Tulipa gesneriana* petals that were subjected to dielectric measurements. These protoplasts are composed of a large vacuole and a thin cytoplasmic layer, which contains numerous chloroplasts for the *Brassica* protoplasts and various membrane-bounded granules for the *Tulipa* protoplasts. The mean diameter was 33.6  $\mu$ m for *Brassica* protoplasts and 60.2  $\mu$ m for *Tulipa* protoplasts.

### Phenomenological analysis of dielectric data

Fig. 2 shows the dielectric dispersion profiles of the protoplasts. The data are expressed in the forms of  $\epsilon_c$ ,  $\kappa_c$ ,  $\epsilon_c''$ , and  $\Delta\kappa_c''$ .  $\epsilon_c$  and  $\kappa_c$  are the relative permittivity and the conductivity of the protoplasts, respectively.  $\epsilon_c''$  is the imaginary part of the complex relative permittivity of the protoplast defined as  $\epsilon_c'' = \kappa_c/\omega\epsilon_0$ .  $\Delta\kappa_c''$  is the imaginary part of the complex conductivity of the protoplast defined as  $\Delta\kappa_c'' = (\epsilon_c - \epsilon_{ch})\omega\epsilon_0$ , where  $\epsilon_{ch}$  is the limiting relative permittivity of the protoplast at high frequencies. For the *Brassica* protoplasts, the curve of  $\epsilon_c''$  shows two peaks centered at 17 kHz and 1.5 MHz, and a very small shoulder that corresponds to a peak of  $\Delta\kappa_c''$  around 1 MHz. With the *Tulipa* protoplasts, the curve of  $\epsilon_c''$  has two peaks at 5 kHz and 0.4 MHz, and the curve of  $\Delta\kappa_c''$  shows one peak at 0.7 MHz and a small shoulder around 2 MHz. These spectra indicate that there are at least three relaxation processes for both protoplasts. Hence, we tried to fit the observed dielectric dispersions with the following empirical equation consisting of three Cole-Cole dispersion terms (Cole and Cole, 1941).

$$\epsilon_c^* = \epsilon_{ch} + \frac{\Delta\epsilon_1}{1 + (jf/f_{c1})^{1-\alpha_1}} + \frac{\Delta\epsilon_2}{1 + (jf/f_{c2})^{1-\alpha_2}} + \frac{\Delta\epsilon_3}{1 + (jf/f_{c3})^{1-\alpha_3}}. \quad (3)$$

The comparison of the best-fit curves and the experimental data gave excellent agreement below about 100 MHz, as shown in Fig. 2. These three subdispersions are termed  $\beta_1$ -,  $\beta_2$ -, and  $\beta_3$ -dispersion from lower frequency to higher. The best-fit parameters are listed in Table 1. The characteristics of the three subdispersions are summarized as: (a) The magnitude of the  $\beta_1$ - and the  $\beta_2$ -dispersion is much larger than that of the  $\beta_3$ -dispersion, especially for the *Tulipa* protoplast. (b) The  $\beta_1$ - and the  $\beta_2$ -dispersions are more than one decade apart from each other, whereas the  $\beta_2$ - and the  $\beta_3$ -dispersions lie within one decade. (c) Since  $\alpha$  indicates the degree of broadening of dispersion curves, the  $\beta_1$ - and the  $\beta_2$ -dispersion curves are broader than the  $\beta_3$ -dispersion curve.

### Analysis based on electrical cell models

We tested three electrical models for the protoplasts shown in Fig. 3: (a) The single-shell model (S-S model) is the simplest model, in which no internal structure is considered. The core phase corresponds to the cytoplasm and the shell to the plasma membrane. This model has fully explained the dielectric dispersion of spherical intact and ghost erythrocytes with no intracellular structure (Asami et al., 1989; Kaneko et al., 1991). (b) The double-shell model (D-S model) takes into account the large vacuole, which is represented by an internal concentric shell-sphere. This model also has been

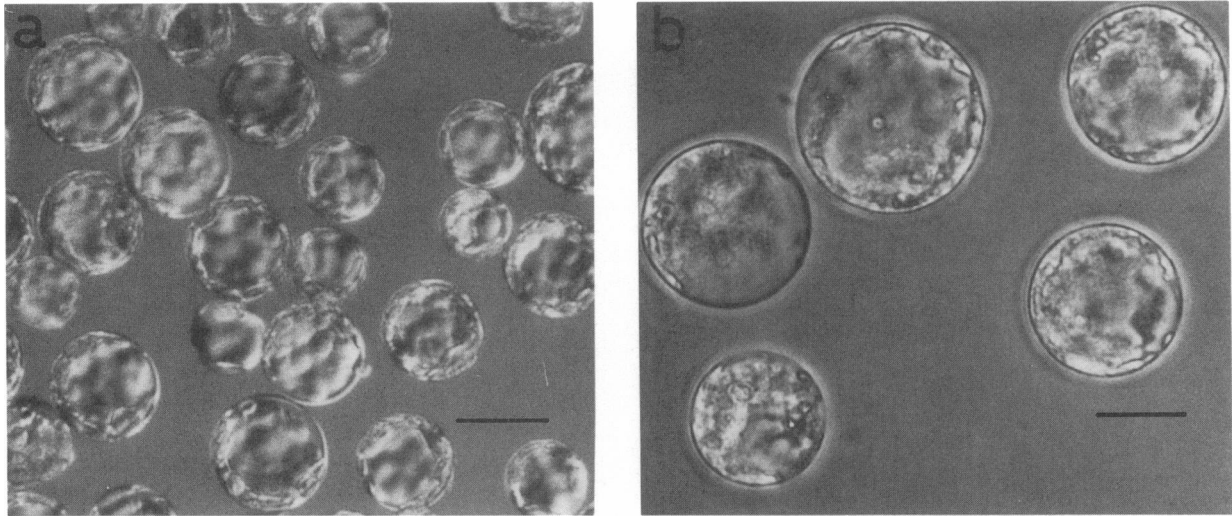


FIGURE 1 Micrographs of (a) *Brassica campestris* leaf protoplasts by differential interference contrast microscopy and (b) *Tulipa gesneriana* petal protoplasts by phase contrast microscopy. Line scale is 30  $\mu\text{m}$ .

applicable to cells containing a sizable nucleus (Irimajiri et al., 1978; Asami et al., 1989) and to intact mitochondria with double membranes (Asami and Irimajiri, 1984). (c) The double-shell model with an intershell space including vesicles (D-S-V model) newly proposed for the protoplast is the most realistic model, which includes both of the vacuole and cytoplasmic organelles.

In the S-S model, a homogeneous sphere (of complex relative permittivity  $\epsilon_i^*$ ) is covered with a shell (of  $\epsilon_m^*$ ). The equivalent, homogeneous complex relative permittivity of the shell-sphere (of  $\epsilon_c^*$ ) is given by the equation derived by Maxwell (1873) and Wagner (1914).

$$\epsilon_c^* = \epsilon_m^* \frac{2(1 - v_1)\epsilon_i^* + (1 + 2v_1)\epsilon_m^*}{(2 + v_1)\epsilon_i^* + (1 - v_1)\epsilon_m^*}, \quad (4)$$

where  $v_1 = (1 - d_m/R_o)^3$ ,  $R_o$  is the outer radius, and  $d_m$  is the shell thickness.

The D-S model is regarded as an S-S model whose interior (of  $\epsilon_i^*$ ) is composed of a concentric sphere (of  $\epsilon_v^*$ ) covered with a shell (of  $\epsilon_t^*$ ), and an intershell space (of  $\epsilon_{cp}^*$ ). In this case,  $\epsilon_i^*$  in Eq. 4 is substituted by

$$\epsilon_i^* = \epsilon_{cp}^* \frac{2(1 - v_2)\epsilon_v^* + (1 + 2v_2)\epsilon_t^*}{(2 + v_2)\epsilon_v^* + (1 - v_2)\epsilon_t^*}, \quad (5)$$

where  $v_2 = (R_v/(R_o - d_m))^3$  and  $R_v$  is the radius of the inner shell-sphere. The complex relative permittivity of the inner shell-sphere  $\epsilon_v^*$  is given by

$$\epsilon_v^* = \epsilon_t^* \frac{2(1 - v_3)\epsilon_i^* + (1 + 2v_3)\epsilon_v^*}{(2 + v_3)\epsilon_i^* + (1 - v_3)\epsilon_v^*}, \quad (6)$$

where  $v_3 = (1 - d_t/R_v)^3$  and  $d_t$  is the shell thickness of the inner shell-sphere. The value of  $\epsilon_c^*$  for the D-S model is, thus, calculated from Eqs. 4, 5, and 6.

When the intershell space in the D-S model is filled with a vesicle suspension, the complex relative permittivity

of the intershell space (or the cytoplasm)  $\epsilon_{cp}^*$  in Eq. 5 may be expressed by Hanai's mixture equation (Hanai, 1960) as:

$$\frac{\epsilon_{cp}^* - \epsilon_g^*}{\epsilon_{cs}^* - \epsilon_g^*} \left( \frac{\epsilon_{cs}^*}{\epsilon_g^*} \right)^{1/3} = 1 - P_g, \quad (7)$$

where  $P_g$  is the volume fraction of the vesicles in the intershell space, and  $\epsilon_{cs}^*$  is the complex relative permittivity of the suspending medium (or the cytosol) of the vesicles. The complex relative permittivity of the vesicle (or the granule)  $\epsilon_g^*$  is expressed as:

$$\epsilon_g^* = \epsilon_{gm}^* \frac{2(1 - v_4)\epsilon_{gi}^* + (1 + 2v_4)\epsilon_{gm}^*}{(2 + v_4)\epsilon_{gi}^* + (1 - v_4)\epsilon_{gm}^*}, \quad (8)$$

where  $v_4 = (1 - d_{gm}/R_g)^3$ ,  $\epsilon_{gi}^*$  is the complex relative permittivity of the vesicle interior,  $\epsilon_{gm}^*$  the complex relative permittivity of the vesicle membrane,  $R_g$  the outer radius of the vesicle, and  $d_{gm}$  the shell thickness of the vesicle. The value of  $\epsilon_c^*$  for the D-S-V model is calculated from the combination of Eqs. 4, 5, 6, 7, and 8.

Fig. 4 shows the experimental data and the best-fit theoretical curves calculated by the three models. The S-S model, which predicts a single dispersion under the conditions that  $\kappa_m/\kappa_i \ll 1$  and  $d_m/R_o \ll 1$ , does not essentially fit the observed dielectric dispersions with three subdispersions. Thus the data only in the  $\beta_1$ -dispersion region were fitted with the S-S model in the following procedure, which is similar to that described by Hanai et al. (1975). First, we chose the value of  $\epsilon_m$  to fit the calculated value of  $\epsilon_{c1}$  (the limiting value of  $\epsilon_c$  at low frequencies) to the measured value. Similarly, we chose the value of  $\epsilon_i$  for the measured values of  $\epsilon_{1-2}$  (the intermediate value of  $\epsilon_c$  between the  $\beta_1$ - and  $\beta_2$ -dispersion) and finally we chose the value of  $\kappa_i$  for the measured value of  $f_{c1}$ . Table 2 shows the estimated best-fit electrical parameters. The capacitance of the plasma membrane, which

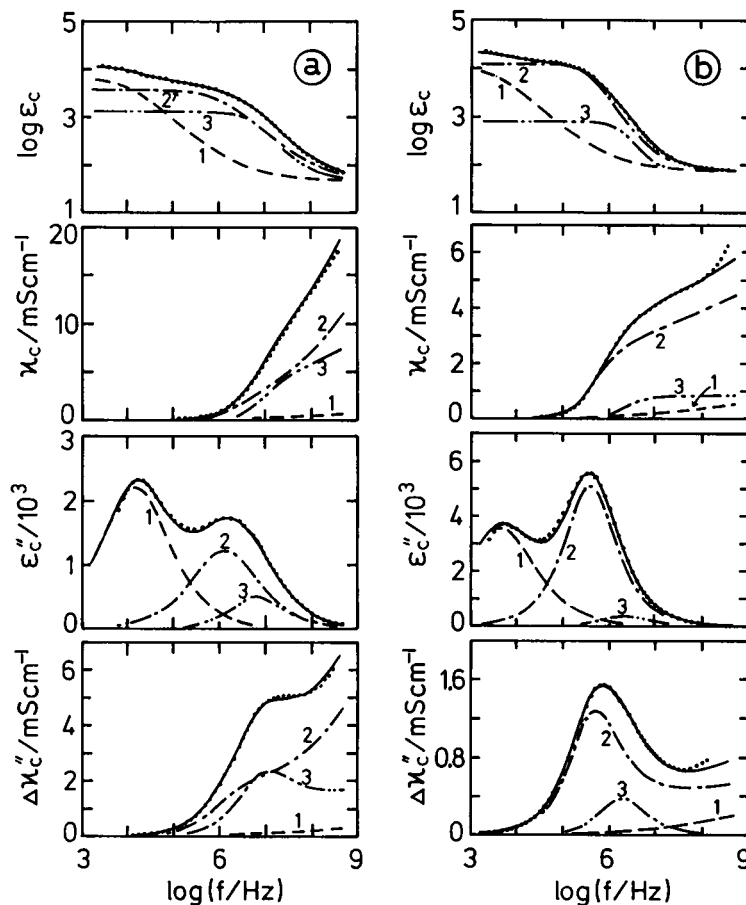


FIGURE 2 Frequency dependence of  $\epsilon_c$ ,  $\kappa_c$ ,  $\epsilon_c''$ , and  $\Delta\kappa_c''$  of (a) *Brassica* protoplasts and (b) *Tulipa* protoplasts. The equivalent, homogeneous complex relative permittivity of the protoplasts ( $\epsilon_c^* = \epsilon_c' - j\epsilon_c'' = \epsilon_c - j\kappa_c/\omega\epsilon_0$ ) was calculated from the complex relative permittivity of the protoplast suspensions using Hanai's mixture equation (Eq. 1).  $\epsilon_c$  and  $\kappa_c$  are the relative permittivity and conductivity of the protoplasts.  $\epsilon_c''$  is the imaginary part of  $\epsilon_c^*$ ;  $\Delta\kappa_c''$  is the imaginary part of the complex conductivity of the protoplasts ( $\kappa_c^* = j\omega\epsilon_c^*$ ) defined as  $\Delta\kappa_c'' = \omega\epsilon_0(\epsilon_c - \epsilon_{ch})$ . The dotted lines indicate experimental data. The solid lines are calculated from Eq. 3 using the best-fit parameters listed in Table 1, being the summation of three sub-dispersions:  $\beta_1$ -dispersion (curve 1),  $\beta_2$ -dispersion (curve 2), and  $\beta_3$ -dispersion (curve 3).

was calculated from  $C_m = \epsilon_m\epsilon_0/d_m$ , was 0.6–0.7  $\mu\text{F}/\text{cm}^2$ . The protoplast interior has extraordinarily high relative permittivity and low conductivity compared with the external medium ( $\epsilon_a = 78$  and  $\kappa_a = 3 \text{ mS}/\text{cm}$ ). This result indicates that a large portion of the protoplast interior is occupied by a membranous structure, which causes the Maxwell–Wagner dispersion.

The D-S model, taking into account a sizable vacuole in the protoplast interior, gave better simulations than

did the S-S model, but there still remained a considerable difference between the observed and calculated data at frequencies above a few MHz. The curve-fitting was made with the data in the  $\beta_1$ - and  $\beta_2$ -dispersion region in a manner analogous to that used for the S-S model. First, we used the same value of  $\epsilon_m$  determined using the S-S model. The value of  $\epsilon_{c1}$  is not changed by the following steps. Next, we chose the value of  $\epsilon_1$  to fit the calculated value of  $\epsilon_{1-2}$  to the measured one. Then we chose the

TABLE 1 Dielectric parameters obtained by fitting Eq. 3, including three Cole–Cole dispersion terms, to dielectric data observed for plant protoplasts

	$\epsilon_{ch}$	$\beta_1$ -dispersion			$\beta_2$ -dispersion			$\beta_3$ -dispersion		
		$\Delta\epsilon_1$	$f_{c1}$	$\alpha_1$	$\Delta\epsilon_2$	$f_{c2}$	$\alpha_2$	$\Delta\epsilon_3$	$f_{c3}$	$\alpha_3$
		$10^3$	kHz		$10^3$	MHz		$10^3$	MHz	
<i>Brassica</i>	48	6.8	15	0.26	3.7	1.36	0.25	1.3	6.4	0.13
<i>Tulipa</i>	72	10.8	4.5	0.26	11.6	0.39	0.08	0.7	2.0	0.01

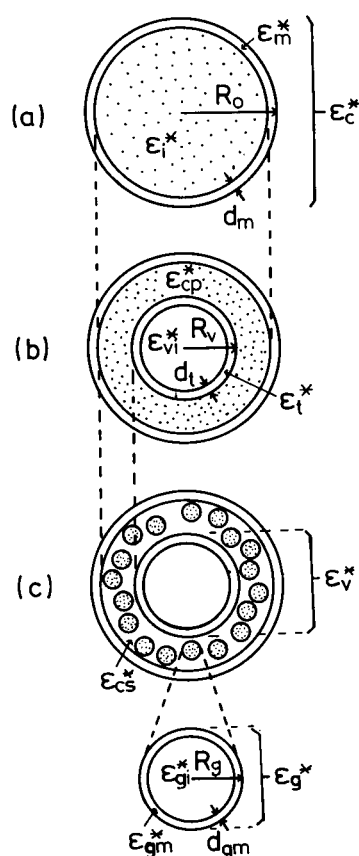


FIGURE 3 Electrical models of protoplasts. (a) Single-shell model (S-S model), (b) Double-shell model (D-S model), (c) Double-shell model with an intershell space including vesicles (D-S-V model). Symbols:  $\epsilon^*$  is complex relative permittivity;  $R_o$ , outer radius;  $R_v$ , vacuole radius;  $R_g$ , vesicle radius;  $d_m$ ,  $d_t$ , and  $d_g$  are thickness of plasma membrane, tonoplast, and vesicle membrane, respectively. Subscripts: m refers to plasma membrane; i cell interior; cp cytoplasm; t tonoplast; vi vacuole space; cs cytosol; gm membrane of cytoplasmic organella; gi interior of cytoplasmic organella; c whole protoplast; v vacuole including tonoplast; g whole organella.

value of  $\epsilon_{cp}$  for the measured value of  $\epsilon_{2-3}$  (the intermediate value of  $\epsilon_c$  between the  $\beta_2$ - and the  $\beta_3$ -dispersion). Finally, we determined the value of  $\kappa_{vi}$  for the measured value of  $f_{c2}$ . The above steps were then repeated several times to obtain good agreement between the calculated and observed dielectric parameters. The electrical parameters thus estimated for the D-S model are listed in Table 3. The capacitance of the tonoplasts was slightly higher than that of the plasma membranes. The relative permittivity of the intershell space was unusually high ( $3-5 \times 10^3$ ), which indicates the interfacial polarization effect due to the cytoplasmic organelles.

The D-S-V model, further taking account of the cytoplasmic organelles, provided much better simulations than did the D-S model, especially in the  $\beta_3$ -dispersion region. The curve-fitting procedure with the D-S-V model was as follows: First, we used the same values of  $\epsilon_m$  and  $\epsilon_t$  determined with the D-S model. The values of  $\epsilon_{c1}$  and  $\epsilon_{1-2}$  are little affected by the next steps. Next, we

chose the values of  $\epsilon_{gm}$  to fit the calculated value of  $\epsilon_{2-3}$  to the measured one. Finally, we chose the values of  $\kappa_{cs}$  and  $\kappa_{gi}$  to fit the calculated data to the measured data in the  $\beta_3$ -dispersion region. The best-fit parameters of the D-S-V model are listed in Table 4. This analysis provides only rough estimates for the electrical parameters of the cytoplasmic organelles because of the lack of accurate information on their morphological parameters and their volume fraction in the cytoplasm. However, the

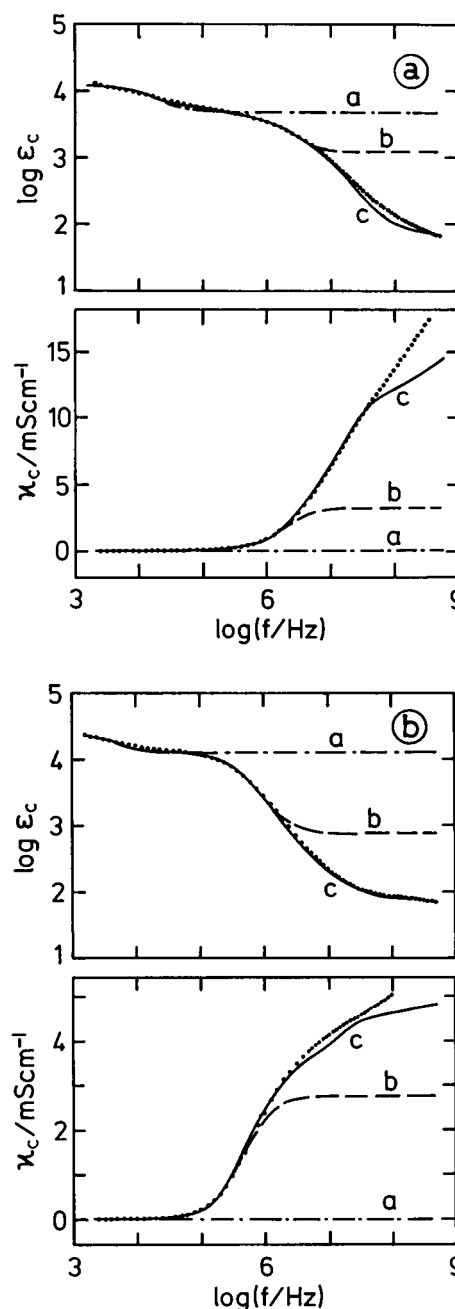


FIGURE 4 Comparison of the experimental data (dotted line) with the theoretical curves calculated using the S-S model (curve a), the D-S model (curve b), and the D-S-V model (curve c). (a) *Brassica* protoplasts, (b) *Tulipa* protoplasts.

TABLE 2 Electrical phase parameters of protoplasts estimated using single-shell model (S-S model)

	$C_m$	$\epsilon_i$	$\kappa_i$
	$\mu\text{F}/\text{cm}^2$	$10^3$	$\text{mS}/\text{cm}$
<i>Brassica</i>	0.62	8.7	0.18
<i>Tulipa</i>	0.68	26.5	0.13

Mean radius of the protoplasts  $R_o$  is 16.8  $\mu\text{m}$  for *Brassica* protoplasts and 30.2  $\mu\text{m}$  for *Tulipa* protoplast. The capacitance of plasma membrane  $C_m$  was calculated from  $C_m = \epsilon_m \epsilon_o / d_m$ . Assumed parameters:  $d_m = 7$  nm, and  $\kappa_m < 10^{-5}$  mS/cm.

estimated values of the membrane capacitance of the chloroplasts and granules ( $1 \mu\text{F}/\text{cm}^2$ ) are reasonable as biological membranes. There still remains a slight discrepancy between the calculated and observed data; the observed curves are broader than the theoretical curves. The broadening of the dispersion curves may be caused by the distributions of the morphological and electrical parameters of the protoplasts, i.e., the variation of the parameters from protoplast to protoplast.

## DISCUSSION

### Dielectric behavior of plant protoplasts

We applied the suspension method (or dielectric spectroscopy) to the highly vacuolated protoplasts isolated from leaves and petals, and found a dielectric dispersion composed of three subdispersions: two large dispersions, and a small one. This dielectric behavior is quite different from that of animal cells, which generally provide one large dispersion and a very small additional one (Irimajiri et al., 1987; Asami et al., 1989). This is attributed to the difference in intracellular structure, i.e., the plant protoplasts have a large vacuole and their cytoplasm includes chloroplasts (or granules) at a high concentration. The spherical cell model taking into account a large vacuole and cytoplasmic organelles, satisfactorily simulated the observed dielectric behavior, and provided reasonable values for the electrical parameters of the vacuole and cytoplasmic organelles.

TABLE 3 Electrical phase parameters of protoplasts estimated using double-shell model (D-S model)

	$C_m$	$\epsilon_{cp}$	$\kappa_{cp}$	$C_i$	$\kappa_{vi}$
	$\mu\text{F}/\text{cm}^2$	$10^3$	$\text{mS}/\text{cm}$	$\mu\text{F}/\text{cm}^2$	$\text{mS}/\text{cm}$
<i>Brassica</i>	0.62	3.4	0.42	0.95	5.5
<i>Tulipa</i>	0.68	5.5	1.0	0.91	3.1

The thickness of the cytoplasmic layer was roughly estimated to be 3.5  $\mu\text{m}$  for *Brassica* protoplasts and 2.0  $\mu\text{m}$  for *Tulipa* protoplasts. The capacitance of tonoplast  $C_i$  was calculated from  $C_i = \epsilon_i \epsilon_o / d_i$ . Assumed electrical parameters:  $\epsilon_{vi} = 75$  and  $\kappa_m = \kappa_i < 10^{-5}$  mS/cm. Assumed morphological parameters:  $d_m = d_i = 7$  nm.

TABLE 4 Electrical phase parameters of protoplasts estimated using double-shell model with an intershell space including vesicles (D-S-V model)

	$C_m$	$\kappa_{cs}$	$C_i$	$\kappa_{vi}$	$C_{gm}$	$\kappa_{gi}$
	$\mu\text{F}/\text{cm}^2$	$\text{mS}/\text{cm}$	$\mu\text{F}/\text{cm}^2$	$\text{mS}/\text{cm}$	$\mu\text{F}/\text{cm}^2$	$\text{mS}/\text{cm}$
<i>Brassica</i>	0.62	3.2	0.95	5.5	1	30
<i>Tulipa</i>	0.68	7.5	0.91	4.0	1	10

The radius of cytoplasmic organelles was roughly estimated as:  $R_g = 2.5 \mu\text{m}$  for chloroplasts in *Brassica* protoplast,  $R_g = 0.8 \mu\text{m}$  for granules in *Tulipa* protoplast. The capacitance of organella membrane was calculated from  $C_{gm} = \epsilon_{gm} \epsilon_o / d_{gm}$ . Assumed electrical parameters:  $\epsilon_{vi} = 75$ ,  $\epsilon_{cs} = 65$ ,  $\epsilon_{gi} = 65$ , and  $\kappa_m = \kappa_i = \kappa_{gm} < 10^{-5}$  mS/cm. Assumed morphological parameters:  $d_m = d_i = d_{gm} = 7$  nm and  $P_g = 0.75$ .

### Electrical parameters of protoplasts

Specific membrane capacitance  $C_m$  has been determined for the plasma membranes of various plant protoplasts by the electrorotation method and dielectrophoresis as follows: 0.48  $\mu\text{F}/\text{cm}^2$  (Arnold and Zimmermann, 1982); 0.24–0.40  $\mu\text{F}/\text{cm}^2$  (Glaser et al., 1983); and 0.24–0.56  $\mu\text{F}/\text{cm}^2$  (Gimsa et al., 1985) by the electrorotation method; and 0.56  $\mu\text{F}/\text{cm}^2$  (Lovelace et al., 1984) and 0.47  $\mu\text{F}/\text{cm}^2$  (Kaler and Jones, 1990) by dielectrophoresis. These values were slightly lower than those estimated in this study (0.62 and 0.68  $\mu\text{F}/\text{cm}^2$ ). In our analysis, the value of  $C_m$  is determined only from the limiting value of  $\epsilon_c$  at low frequencies where  $\epsilon_c$  is not influenced by the dielectric properties of the protoplast interior. Hence, the three spherical models used gave the same values for  $C_m$ .

The capacitance of the tonoplasts (or vacuolar membranes)  $C_i$  was estimated to be about 1  $\mu\text{F}/\text{cm}^2$  for both protoplasts, which is about two times higher than that obtained for the vacuoles isolated from *Avena sativa* by the electrorotation method (Gimsa et al., 1985). Our value also did not agree with that found for the tonoplast of *Nitellopsis obtusa* (2  $\mu\text{F}/\text{cm}^2$ ) (Bernhardt and Pauly, 1974) and for *Valonia utricularis* (4  $\mu\text{F}/\text{cm}^2$ ) (Zimmermann et al., 1982) using microelectrode techniques. The reason for the widely varying value of  $C_i$  from cell to cell is not clear and remains to be solved in the future.

The limiting value of  $\epsilon_c$  at high frequencies  $\epsilon_{ch}$  is a function of the relative permittivities of the vacuolar space  $\epsilon_{vi}$ , the organelle interior  $\epsilon_{gi}$ , and the cytosol  $\epsilon_{cs}$ . When we assumed 60 for  $\epsilon_{gi}$  and  $\epsilon_{cs}$ , the value of  $\epsilon_{vi}$  was calculated from the observed values of  $\epsilon_{ch}$  and was 75 for both protoplasts. The conductivity of the vacuolar space  $\kappa_{vi}$  was 8 mS/cm for *Brassica* protoplasts and 4 mS/cm for *Tulipa* protoplasts. These values for  $\epsilon_{vi}$  and  $\kappa_{vi}$  seem to be reasonable because the vacuolar space is filled with a simple aqueous solution of nutrients, metabolite and inorganic ions, and the total concentration of inorganic ions in vacuole space is comparable to that in the cytosol (Martinoia et al., 1986).

We would like to thank Dr. T. Hanai for his valuable advice and active encouragement.

This research was supported in part by grant 03650791 from the Ministry of Education, Science and Culture, Japan.

Received for publication 1 April 1992 and in final form 14 July 1992.

## REFERENCES

- Arnold, W. M., and U. Zimmermann. 1982. Rotating-field-induced rotation and measurement of the membrane capacitance of single mesophyll cells of *Avena sativa*. *Z. Naturforsch.* 37c:908-915.
- Asami, K. and T. Hanai. 1992. Dielectric monitoring of biological cell sedimentation. *Colloid & Polym. Sci.* 270:78-84.
- Asami, K., and A. Irimajiri. 1984. Dielectric analysis of mitochondria isolated from rat liver. II. Intact mitochondria as simulated by a double-shell model. *Biochim. Biophys. Acta.* 778:570-578.
- Asami, K., A. Irimajiri, T. Hanai, N. Shiraishi, and K. Utsumi. 1984. Dielectric analysis of mitochondria isolated from rat liver. I. Swollen mitoplasts as simulated by a single-shell model. *Biochim. Biophys. Acta.* 778:559-569.
- Asami, K., Y. Takahashi, and S. Takashima. 1989. Dielectric properties of mouse lymphocytes and erythrocytes. *Biochim. Biophys. Acta.* 1010:49-55.
- Bernhardt, J., and H. Pauly. 1974. Dielectric measurements of *Nitellopsis obtusa* cells with intracellular electrodes. *Rad. Environ. Biophys.* 11:91-109.
- Cole, K. S. 1968. *Membranes, Ions and Impulses*. University of California Press, Berkeley and Los Angeles.
- Cole, K. S., and R. H. Cole. 1941. Dispersion and absorption in dielectrics. I. Alternating current characteristics. *J. Chem. Phys.* 9:341-351.
- Foster, K. R., and H. P. Schwan. 1986. Dielectric properties of tissues. In *CRC Handbook of Biological Effects of Electromagnetic Fields*. C. Polk and E. Postow, editors. CRC Press Inc., Boca Raton, FL. 27-96.
- Fuhr, G., J. Gimsa, and R. Glaser. 1985. Interpretation of electrorotation of protoplasts. I. Theoretical considerations. *Stud. Biophys.* 108:149-164.
- Gimsa, J., G. Fuhr and R. Glaser. 1985. Interpretation of electrorotation of protoplasts. II. Interpretation of experiments. *Stud. Biophys.* 109:5-14.
- Glaser, R., G. Fuhr, and J. Gimsa. 1983. Rotation of erythrocytes, plant cells, and protoplasts in an outside rotating electric field. *Stud. Biophys.* 96:11-20.
- Hanai, T. 1960. Theory of the dielectric dispersion due to the interfacial polarization and its application to emulsions. *Kolloid Z.* 171:23-31.
- Hanai, T., N. Koizumi, and A. Irimajiri. 1975. A method for determining the dielectric constant and the conductivity of membrane-bounded particles of biological relevance. *Biophys. Struct. Mech.* 1:285-294.
- Hanai, T., K. Asami, and N. Koizumi. 1979. Dielectric theory of concentrated suspensions of shell-spheres in particular reference to the analysis of biological cell suspensions. *Bull. Inst. Chem. Res., Kyoto Univ.* 57:297-305.
- Irimajiri, A., K. Asami, T. Ichinowatari, and Y. Kinoshita. 1987. Passive electrical properties of membrane and cytoplasm of cultured rat basophil leukemia cells. I. Dielectric behavior of cell suspensions in 0.01-500 MHz and its simulation with a single-shell model. *Biochim. Biophys. Acta.* 896:203-213.
- Irimajiri, A., Y. Doida, T. Hanai, and A. Inouye. 1978. Passive electrical properties of cultured murine lymphoblast (L5178Y) with reference to its cytoplasmic membrane, nuclear envelope, and intracellular phases. *J. Membr. Biol.* 38:209-232.
- Irimajiri, A., T. Hanai, and A. Inouye. 1975. Evaluation of a conductometric method to determine the volume fraction of the suspensions of biomembrane-bounded particles. *Experientia (Basel)*. 31:1373-1374.
- Irimajiri, A., T. Hanai, and A. Inouye. 1979. A dielectric theory of "multi-stratified shell" model with its application to a lymphoma cell. *J. Theor. Biol.* 78:251-269.
- Irimajiri, A., T. Suzuki, K. Asami, and T. Hanai. 1991. Dielectric modeling of Biological cells. Models and Algorithm. *Bull. Inst. Chem. Res., Kyoto Univ.* 69:421-438.
- Kaler, K. V. I. S., and T. B. Jones. 1990. Dielectrophoretic spectra of single cells determined by feedback-controlled levitation. *Biophys. J.* 57:173-182.
- Kaneko, H., K. Asami, and T. Hanai. 1991. Dielectric analysis of sheep erythrocyte ghost. Examination of applicability of dielectric mixture equations. *Colloid & Polym. Sci.* 269:1039-1044.
- Lovelace, R. V. E., D. G. Stout, and P. L. Steponkus. 1984. Protoplast rotation in a rotation electric field: the influence of cold acclimation. *J. Membr. Biol.* 82:157-166.
- Martinoia, E., M. J. Schramm, G. Kaiser, W. M. Kaiser, and U. Heber. 1986. Transport of anions in isolated barley vacuoles. I. Permeability of anions and evidence for a Cl<sup>-</sup>-uptake system. *Plant Physiol. (Bethesda)*. 80:895-901.
- Maxwell, J. C. 1892. *Treatise on Electricity and Magnetism*. Clarendon Press, Oxford.
- Pauly, H., and H. P. Schwan. 1959. Über die Impedanz einer Suspension von kugelförmigen Teilchen mit einer Schale. *Z. Naturforsch.* 14b:125-131.
- Pethig, R. 1979. *Dielectric and Electronic Properties of Biological Materials*. John Wiley & Sons, New York.
- Schwan, H. P. 1957. Electrical properties of tissue and cell suspensions. In *Advances in Biological and Medical Physics*. Vol. 5. J. H. Lawrence and C. A. Tobias, editors. Academic Press, New York. 147-209.
- Takashima, S. 1989. *Electrical Properties of Biopolymers and Membranes*. Adam Hilger, Bristol, England. 143-193.
- Takebe, I., Y. Otsuki, and S. Aoki. 1968. Isolation of tobacco mesophyll cells in intact and active state. *Plant Cell Physiol.* 9:115-124.
- Wagner, K. W. 1914. Erklärung der dielektrischen Nachwirkungsvorgänge auf Grund Maxwellscher Vorstellungen. *Archiv für Elektrotechnik* 2:371-387.
- Zimmermann, U., K. H. Büchner, and R. Benz. 1982. Transport properties of mobile charges in algal membranes: Influence of pH and turgor pressure. *J. Membr. Biol.* 67:183-197.